Dynamic *in situ* optical and magneto-optical monitoring of the growth of Co-Pd multilayers

2001 J. Phys.: Condens. Matter 13 691

(http://iopscience.iop.org/0953-8984/13/4/315)

INSTITUTE OF PHYSICS PUBLISHING JOURNAL OF PHYSICS: CONDENSED MATTER

J. Phys.: Condens. Matter **13** (2001) 691–705 www.iop.org/Journals/cm PII: S0953-8984(01)16555-0

Dynamic *in situ* optical and magneto-optical monitoring of the growth of Co–Pd multilayers

R Atkinson[1], **G Didrichsen, W R Hendren, I W Salter and R J Pollard**

The Queen's University of Belfast, Department of Pure and Applied Physics, Belfast BT7 1NN, UK

E-mail: ronald.atkinson@qub.ac.uk

Received 21 August 2000, in final form 21 November 2000

Abstract

In situ ellipsometry and Kerr polarimetry have been used to follow the continuous evolution of the optical and magneto-optical properties of multiple layers of Co and Pd during their growth. Films were sputter deposited onto a Pd buffer layer on glass substrates up to a maximum of $N = 10$ bi-layer periods according to the scheme glass/Pd(10)$N \times$ (0.3Co/3Pd) (nm). Magnetic hysteresis measurements taken during the deposition consistently showed strong perpendicular anisotropy at all stages of film growth following the deposition of a single monolayer of Co. Magneto-optic signals associated with the normal-incidence polar Kerr effect indicated strong polarization of Pd atoms at both Co–Pd and Pd–Co interfaces and that the magnitude of the complex magneto-optic Voigt parameter and the magnetic moment of the Pd decrease exponentially with distance from the interface with a decay constant of 1.1 nm^{-1}. Theoretical simulations have provided an understanding of the observations and allow the determination of the ultrathin-film values of the elements of the skew-symmetric permittivity tensor that describe the optical and magneto-optical properties for both Co and Pd. Detailed structure in the observed Kerr ellipticity shows distinct Pd-thickness-dependent oscillations with a spatial period of about 1.6 nm that are believed to be associated with quantum well levels in the growing Pd layer.

1. Introduction

There has been considerable attention given recently to the optical, magneto-optical and magnetic properties of multilayered systems, where individual films are typically a few atoms thick [1–5]. This is particularly true for next-generation magneto-optic recording media. It is intuitively obvious that the electronic structures of very thin films may differ significantly from those of the bulk and that this may be reflected in the physical properties of the material, including the optical, magneto-optical and magnetic properties [6]. Several theoretical and

[1] Author to whom any correspondence should be addressed; telephone: +44 028 90 273546; fax: +44 028 90 236226.

0953-8984/01/040691+15$30.00

experimental studies have been made of the properties of multilayer systems that show strong evidence for new properties that cannot be explained on the basis of bulk data [7, 8]. In the case of multilayered Co–Pt and Co–Pd a good deal of the magneto-optic activity, especially at short wavelengths, is believed to originate from the polarization of the Pd and Pt atoms at interfaces with Co. However, the magnitude and spatial distribution of this polarization is not well understood or characterized. In addition, it is not easy to model the behaviour of such systems because there have been no direct measurements of the fundamental parameters that describe the magneto-optical behaviour of the materials in their ultrathin-film form—particularly when they are in close proximity to each other, such as at interfaces.

The authors have recently carried out a comprehensive study of the growth of several multilayer systems using *in situ* optical, magneto-optical and magnetic diagnostics to follow the evolving properties of such structures in real time. During these studies it has become clear that the Co–Pd and Co–Pt systems are very different both in their growth mechanisms and their magneto-optical and magnetic properties. The Co–Pd system is particularly well behaved as regards its physical growth and the magneto-optical signals that are produced during a typical deposition sequence. These can be modelled on the basis of theoretical calculations that take into account the inhomogeneous nature of the polarization of the layers. Such calculations are carried out using the fundamental optical and magneto-optical constants of the materials. These are the complex refractive index n $(=n' + \mathrm{i}n'')$ and the complex magneto-optic Voigt parameter Q $(=Q_1 + \mathrm{i}Q_2)$ that appears as an off-diagonal component in the skew-symmetric tensor of a gyroelectric medium [9]. In this paper we report on the observations and analysis of the growth of several Co–Pd multilayers. From the extensive data that have been produced we have been able to deduce the optical and magneto-optical parameters of both materials for thicknesses in the range 0–3 nm and, more importantly in the case of Pd, have been able to determine the distribution of the polarization in a direction perpendicular to the growth plane.

Although the level of agreement between observations and calculated data is excellent, there are some very small systematic differences that cannot easily be explained in terms of the usual optical and magneto-optical parameters. In particular we have evidence, for the first time, that thickness-dependent oscillations occur in the Co–Pd system during the deposition of the Pd layer and that it is very likely that these are related to electronic transitions to quantum well states in the Pd that are also thickness dependent.

2. Experimental procedure

Figure 1 shows a schematic diagram of the deposition chamber and associated monitoring equipment. Two, PC-controlled, planar RF magnetrons were used to sputter deposit multiple layers of Co and Pd onto glass substrates at room temperature in an argon pressure of $\sim 2.2 \times 10^{-3}$ mbar.

In situ optical and magneto-optical monitoring, at a wavelength $\lambda = 632.8$ nm, was achieved using a fast, rotating-analyser ellipsometer and a normal-incidence Kerr polarimeter. The ellipsometer, operating at an angle of incidence of 70°, was used to determine the optical functions $\mathrm{Re}(r_p/r_s)$ and $\mathrm{Re}(r_s/r_p)$, where r_p, r_s are the complex Fresnel-amplitude reflection coefficients for p- and s-polarized light, respectively. Complete data sets were obtained each second, during the deposition period. Individual measurements were completed within 100 ms.

The Kerr polarimeter, based on the use of a photoelastic modulator (PEM) operating at 50 kHz, allowed the simultaneous measurement of both Kerr rotation and ellipticity with precisions better than ±1 arcsecond, limited by mechanical vibrations rather than shot noise or laser instabilities. The details of this technique have been well described previously [10]. It was ensured that radiation incident on the sample was linearly polarized by the use of an

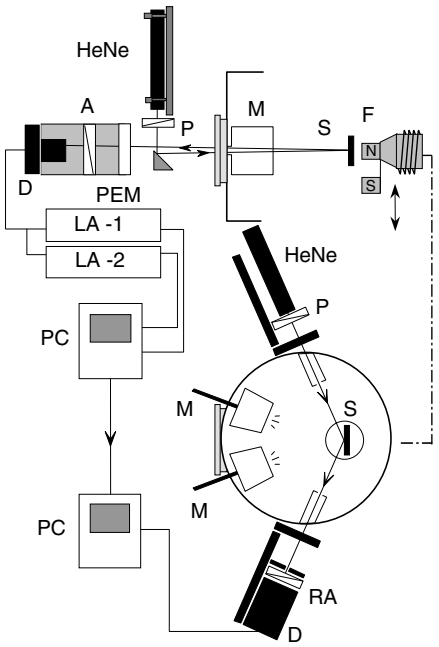

Figure 1. A schematic diagram of the deposition system. HeNe: helium–neon laser; A: analyser; P: polarizer; RA: rotating analyser; PEM: photoelastic modulator; M: magnetron; PC: computer; S: substrate; D: detector; LA-1: lock-in amplifier (50 kHz); LA-2: lock-in amplifier (100 kHz); F: field switch /electromagnet.

aluminium reflector and the choice of the orientation of the primary polarizer with respect to the plane of incidence of the mirror reflecting the beam into the system. All films were deposited in an applied perpendicular field of 0.28 T, produced by permanent magnets that could be reversed automatically if required. All optical windows into the vacuum system were manufactured, in-house, from carefully selected low-stress-optical-coefficient glass. To examine the magnetic properties, during deposition, a variable-field electromagnet was used together with the Kerr signal to plot perpendicular hysteresis loops. In order to do this, the deposition was interrupted for a period of $\sim$120 s. Two synchronized computers coordinated the complete deposition sequence. These controlled mechanical aspects, such as magnetron shutters, magnetic field switching and control and the status of a quartz crystal monitor as well as the operation of the ellipsometer and all data collection during the deposition.

Figure 2 illustrates the XRD pattern that is typical of the Co–Pd multilayers deposited in this series of experiments. Given the low number of bi-layers and the single monolayer of cobalt, the appearance of low- and high- (inset) angle peaks associated with the bi-layer periodicity confirms a well defined layered structure. Strong Kiessig fringes also indicate the existence of sharp interfaces on both sides of the multilayer.

3. Optical results

In this, and section 4, we present both the ellipsometric and magneto-optical data as functions of time or film thickness during the deposition of $N \times$ (CoPd) bi-layers on a 10 nm Pd buffer layer on glass. It is emphasized that the observations are typical and have been repeated several times with good reproducibility.

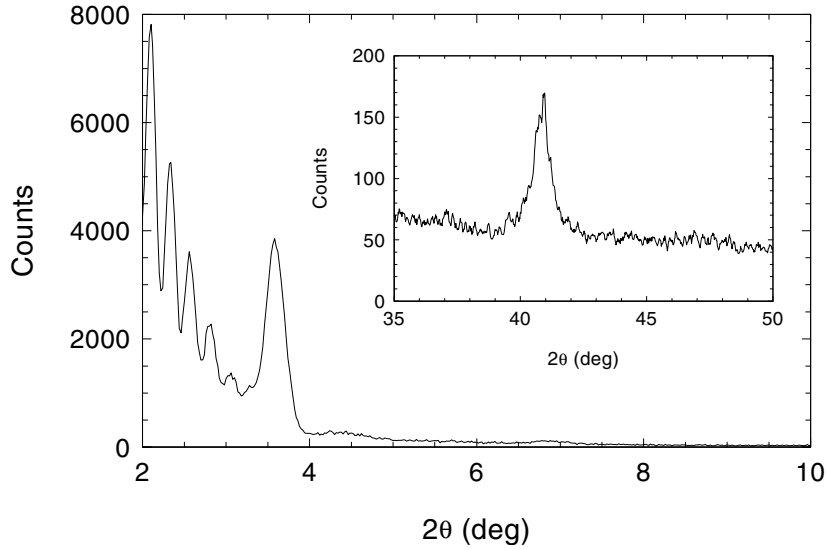

Figure 2. Typical low-angle and (inset) high-angle XRD peaks for Co/Pd multilayers on a 10 nm Pd buffer layer on glass.

Figure 3 shows the evolving optical properties of the buffer layer and the first six periods of the multilayer. At the end of the deposition the total thickness of the film is greater than the optical skin depth for the material. Consequently, the variations in the ellipsometric functions are minimal beyond this point. The continuous curves in this figure are the real-time data traces taken during the deposition process. For the bulk form, the complex refractive indices of Co and Pd are not too dissimilar and as a consequence of this, and the fact that the greater part of the system is composed of Pd, the evolving optical properties are not particularly revealing. However, it is worth pointing out the rapid variations seen during the deposition of the buffer

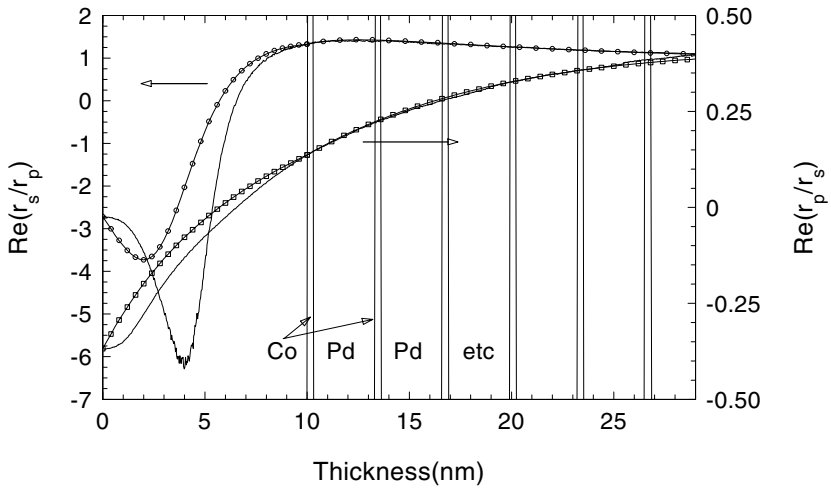

Figure 3. Ellipsometric measurements at $\lambda = 632.8$ nm, for glass/Pd(10)6 $\times$ (0.3Co/3Pd) (nm) as a function of increasing total film thickness. (Calculated curves are shown with markers).

layer. In part, these are a consequence of the optical constants of Pd that can, for example, be deduced from the ellipsometric data at the end of the buffer layer deposition. Such a calculation leads to a value of n_{Pd} (=2.20 + i 3.99) and this may be used to predict the details of the curves corresponding to this initial layer. The predicted curves are also shown, with markers, in figure 3. It will be noticed that whilst the general shape of the curves is correct, the details are not in agreement, particularly in the case of $\mathrm{Re}(r_s/r_p)$. The reason for this is well understood and is related to the ultrathin nature of the film and/or the difficulties of nucleating the film of Pd on the glass substrate surface. Depending upon the nature of the nucleation process, the characteristic optical signatures can often be modelled using an effective medium [11] or Maxwell-Garnett [12] model of the growing film. This can be done quite successfully, for example, for Au films nucleating on glass substrates [13]. However, these observations are not an essential or important feature of this particular work and for this reason are not considered further.

Beyond the buffer layer, growth proceeds as each consecutive bi-layer period is deposited. It can be seen clearly from figure 3 that the ellipsometric functions change monotonically from the buffer layer indicating a stable optical character for the multilayered medium that does not alter significantly during the deposition of the two different materials. This can be examined in more detail in figure 5 which shows a magnified section of the process where the most rapidly changing function $\mathrm{Re}(r_p/r_s)$ is displayed as a function of deposition time. For this particular deposition, a time delay of 80 s was deliberately inserted after the Co layer had been deposited.

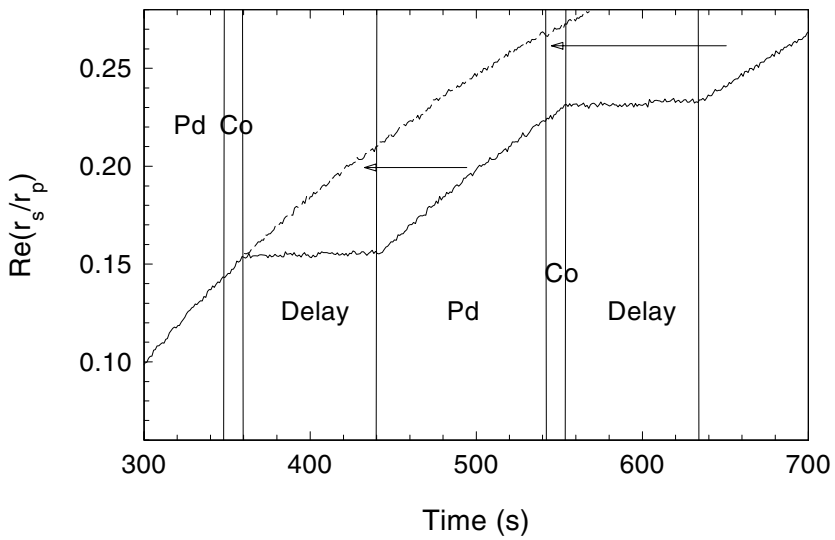

Figure 4. Detail of the temporal variations of the ellipsometric measurements of $\mathrm{Re}(r_s/r_p)$ at $\lambda = 632.8$ nm. The dotted section corresponds to the removal of the time delay periods.

There are two important features of this curve that should be noted. First, it is clear that during the time delay period the optical signals are quite stable. This is important since it indicates that the optical measurement system is reliable and suffers from no significant instrumental drift. In addition, it may also indicate that the physical film system does not suffer from any interdiffusion of Co into the Pd. The latter point should however be qualified by saying that, because of the similarities in the optical properties of the two materials, no great changes in the ellipsometric data would be expected if alloying was taking place. This point is discussed later. Second, if the delay periods are removed from the process, the evolving

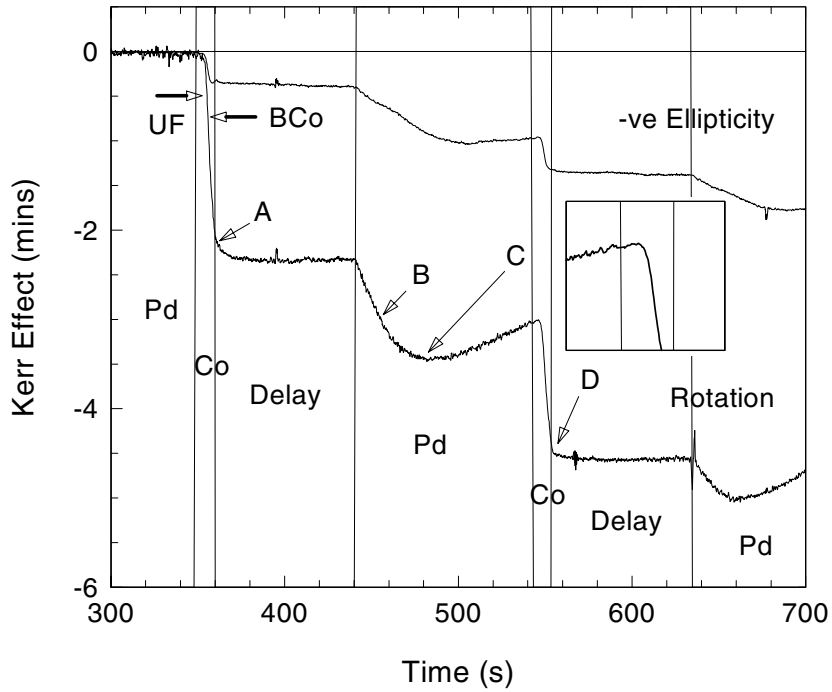

Figure 5. Temporal variations of the complex magneto-optic effect during the deposition of the buffer layer and first two bi-layers of Co–Pd. The inset is a magnified view of the knee between C and D.

curves show no indication of any changes that would indicate the deposition of the different materials. This is illustrated in figure 4 by the dashed curve that corresponds to the removal of the time delay sections.

The smooth continuous character of this curve, which applies to all other optical data, is very important since it allows us to treat the multilayer structure as a homogeneous optical system with a single, spatially independent, refractive index. This is despite the fact that the system is physically and, as we shall see later, magnetically inhomogeneous. The effective single refractive index of the multilayer may be easily determined from the ellipsometric data of figure 3 and is given in table 1. The fact that a single value of the refractive index applies to the whole system may be seen from the calculated curves shown with markers in figure 3 for the section corresponding to the deposition of the six bi-layer periods. The calculated curves are obtained by treating the whole multilayer as a single film of increasing thickness but fixed

Table 1. Optical, magneto-optical and decay parameters at $\lambda = 632.8$ nm determined in this work and used in theoretical calculations.

Layer type	Refractive index (± 0.002)	Q	β (nm^{-1})
Incident medium	1	0	
Co	$2.333 + i\,4.112$	$-0.0126 + i\,0.0007$	0
Pd	$2.333 + i\,4.112$	$-0.0025 + i\,0.0200$	1.1 ± 0.1
Substrate glass	1.519	0	

refractive index. The curves can be seen to fit very well indeed and also fit, equally well, up to the tenth and final bi-layer—though this is not shown since it would reduce the clarity of the detail seen in the curves presented.

4. Magneto-optical observations

Magneto-optical measurements of the polar Kerr rotation (θ_k) and ellipticity (ε_k) were also taken simultaneously and continuously throughout the deposition and, where appropriate, the deposition could be briefly interrupted in order for magnetic hysteresis loops to be plotted. In general, depositions were continuous with time delays inserted after some layer depositions if required. Again it is worth pointing out that many depositions were made and the reproducibility was found to be excellent. In examining the following data the reader should note that the preferred sign convention for magneto-optical effects and parameters has been adopted and is fully defined elsewhere [14].

Figure 5 shows the magneto-optic data corresponding to the first two bi-layers where a time delay of 80 s was incorporated after the Co layers were deposited. Before discussing these data in detail it is important to establish the magnetic properties of the growing films at various stages of the deposition. Although figure 5 corresponds to a continuous process, other depositions have enabled the determination of the hysteresis loops at various points. These are marked A–D in figure 5 and the corresponding loops are shown in figure 6. The important features of these loops are that strong perpendicular anisotropy is developed immediately upon the formation of a continuous Co monolayer and that this is maintained during the subsequent addition of the Pd overlayer. The result is a square, easily saturated, loop at all important stages

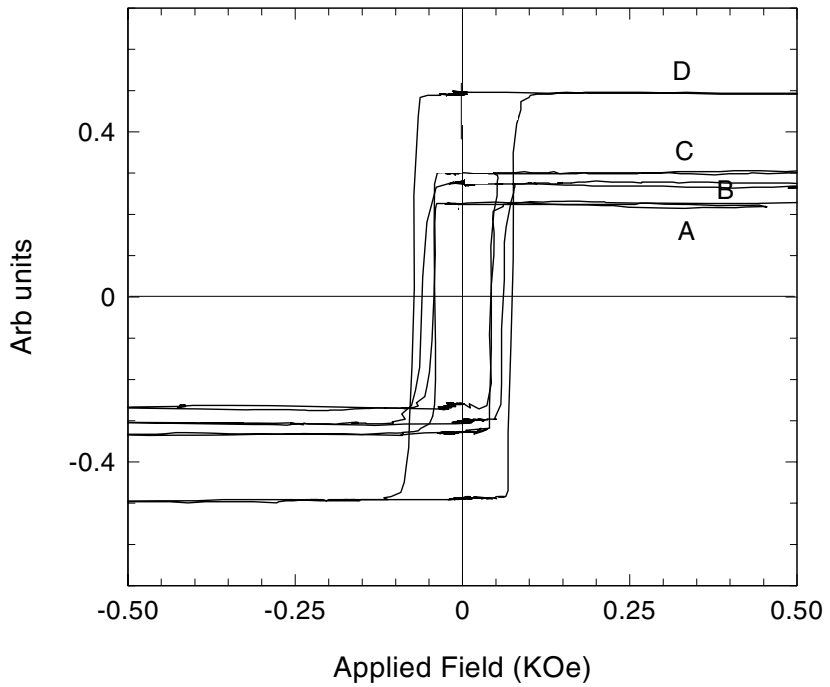

Figure 6. Perpendicular magneto-optic hysteresis loops corresponding to the positions marked A–D in figure 5.

of deposition and for this reason one may assume that all magneto-optic data collected during the process correspond to the film having saturated magnetization, perpendicular to the film plane. In addition, a field of 0.28 T was applied during film growth and was only switched briefly, every third bi-layer, to check for any instrumental drift due to mechanical movement. Normally there was none.

On the basis of the optical and magnetic properties described, the curves of figure 5 may be interpreted in terms of the varying magneto-optical parameters of the growing films. It should be remembered that the material optical properties are homogeneous and unchanging. As regards figure 5 a number of features of the curves are worth noting and these are enumerated below.

(1) On the deposition of the Co monolayer there is a large increase in both Kerr rotation and ellipticity, the former being larger than the latter by a factor of about 4.
(2) The onset of magneto-optic activity of the Co does not occur until approximately 0.14 nm has been deposited.
(3) During the time delay of 80 s the magneto-optical signals remain stable showing no signs of drift or changing magnetic properties.
(4) On deposition of the Pd there is an initial increase in magneto-optic signal that reaches maximum amplitude before reducing towards zero.
(5) The noise on the rotation signal is larger than that on the ellipticity since the latter is a phase-dependent measurement and, naturally, not affected by system vibrations to the same extent as rotation.

Before giving a detailed analysis of these curves there are several points that should be emphasized.

First, on the deposition of the completed cobalt layer the increase of Kerr rotation and ellipticity is much greater than one would expect on the basis of the magneto-optical parameters of ultrathin-film cobalt or even on the basis of the parameters of bulk Co [15]. The former have been deduced from *in situ* experiments on Co–Au multilayers [16] and the predicted Kerr rotation in a situation where the Pd is unpolarized is marked ('UF') on figure 5. For comparison, the value corresponding to bulk cobalt properties is also shown ('BCo').

Second, the increase in magneto-optic activity during the deposition of the Co monolayer is greater than that which occurs on the deposition of the following Pd. In fact, the activity expected from a monolayer of Co, plus that associated with the Pd overlayer, more or less accounts for the total activity seen on the deposition of the Co layer alone. This is indisputable evidence for the polarization of the Pd both below, and above, the Co.

Third, it should be noted that during the deposition of the first 0.14 nm of cobalt the layer remains non-ferromagnetic. This is understandable since ferromagnetism is a collective phenomenon and therefore requires a minimum number of assembled atoms to show the effect. Below the critical thickness of 0.14 nm, the film is either paramagnetic or in the superparamagnetic state. Above this thickness, it is concluded that cluster formation results in islands big enough to become ferromagnetic. This aspect of the data is illustrated in the magnified inset of figure 5 where the onset of the ferromagnetic state is clearly preceded by the deposition of a non-magnetic Co that only adds optical absorption to the system and, as a consequence, a decrease in the magneto-optic signals. This results in an associated decrease in observed magneto-optical activity prior to an increase when the ferromagnetic state becomes active. It is worth pointing out that this phenomenon is observed during the growth of both CoAu [16] and CoPt multilayers. An alternative explanation is that the sub-monolayer film is ferromagnetic but has poorly developed perpendicular anisotropy. However, given repeated observations on three different material systems in an applied field of 0.28 T, it is felt that

this suggested scenario is unlikely. Furthermore, at some point the isolated Co atoms must be non-ferromagnetic.

Fourth, the time delay periods inserted after the Co deposition, though not spectacular in that they show little change, are important for two reasons. They demonstrate the stability of the experimental system and, more importantly, they show that the films are stable magnetically and magneto-optically. It is concluded therefore that there is no significant redistribution or alloying of atoms after the deposition of the Co. Though not shown, a similar stability is seen if time delays are inserted after the deposition of the Pd. Finally, on deposition of Pd there is an initial increase in the magneto-optic signal that decreases after passing though the maximum amplitude. This is clearly due to a magnetically polarized layer whose moment decreases with distance from the interface with Co.

These central observations having been made, it remains to determine the spatial variations of the magneto-optic parameter for this multiple bi-layered system. In the case of the Co monolayer, it is considered to be so thin that only a single magneto-optic parameter can be associated with the completed layer. In the case of the Pd, the variation of the magneto-optic parameter obviously extends over several atomic layers and is decreasing with distance from the interface. For this reason we must deduce both its magnitude and spatial variation. This is important since, assuming that $|Q_{\mathrm{Pd}}|$ is magnetization dependent, we may obtain the normalized spatial dependence of the magnitude of the magnetic moment of Pd atoms when in contact with a Co surface. The absolute magnitude of the moment cannot, of course, be easily determined.

In order to deduce all of these parameters we must fit the complex magneto-optic profiles of the growing films shown in figure 5 to an appropriate model. This can only be done by carrying out magneto-optical calculations for systems having inhomogeneous distributions of magnetization.

5. Theory of inhomogeneous systems

There are several ways of dealing with inhomogeneously magnetized systems. Either one may apply the well known 4×4 matrix approach [17] where each layer is subdivided into elemental layers, or one may determine and apply the special 4×4 characteristic matrix that corresponds to each inhomogeneously magnetized layer and apply this repeatedly in the usual way [18]. In general, the latter approach is particularly tedious. An alternative approach that may be applied in situations where the optical properties are homogeneous throughout the system, which is the case here, relies on the application of the method of differential reflectance [19] combined with the principle of superposition of magneto-optical effects [20]. This states that the magneto-optic Kerr coefficient, k, for any thin-film system is a linear superposition of the elemental Kerr coefficients δk, for individual layers where each value of δk is evaluated assuming that the rest of the film system is non-magnetic. With reference to figure 7 it may be determined that, for the elemental magnetic layer of thickness δz, buried in an optically homogeneous film of thickness d and refractive index n_m, the corresponding Kerr coefficient is

$$\delta k = \mathrm{i}\frac{\delta r}{2}. \tag{1}$$

δr $(=r_+ - r_-)$ is the differential reflectance corresponding to the two refractive indices n_+ and n_- $(n_\pm = n_m(1 \pm \mathrm{i}Q(z)/2))$, that apply at normal incidence to the two magneto-optic, counter-rotating, circularly polarized modes associated with the polar effect. By integrating the elemental Kerr coefficient over the thickness of the film, having a spatially z-dependent magneto-optic parameter $Q(z)$, the total Kerr component can be determined. The detailed

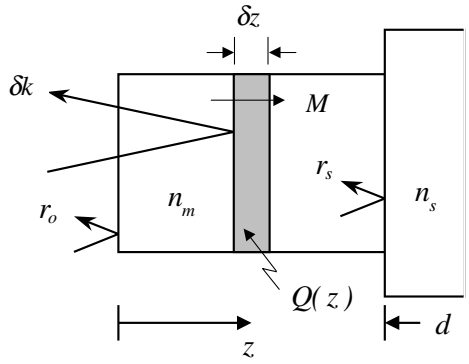

Figure 7. A schematic diagram of an elemental film of thickness δz and magnetization M buried in an optically homogeneous layer on a substrate.

expression for δk is obtained using the repeated application of the reiterative reflectance formula, assuming that $Q(z) \ll 1$. The integrated result is

$$k = \int_0^d \mathrm{d}k = \int_0^d B_0 Q(z)[1 + B_1 \mathrm{e}^{-2\alpha z} + B_2 \mathrm{e}^{-\alpha z}]\alpha \mathrm{e}^{\alpha z}\, \mathrm{d}z \tag{2}$$

where

$$B_0 = \mathrm{i}n_m/((1 + n_m)(1 + r_o r_s \mathrm{e}^{\alpha d}))^2 \tag{3}$$

$$B_1 = r_s^2 \mathrm{e}^{2\alpha d} \tag{4}$$

$$B_2 = 2r_s \mathrm{e}^{\alpha d} \tag{5}$$

and

$$\alpha = \mathrm{i}\, 4\pi n_m/\lambda. \tag{6}$$

B_0, B_1 and B_2 are optical functions with r_o and r_s being the Fresnel-amplitude reflection coefficients at semi-infinite boundaries at the incident and substrate media, respectively, and λ is the free-space wavelength. Perhaps the most significant factor in this expression is $Q(z)$, since this represents the variation of the magneto-optic parameter as a function of distance z perpendicular to the film plane and must take into account the variations within the various layers in the multilayer system. The refractive indices of the incident and substrate media are known and that of the film has been deduced from ellipsometry as previously described. B_0, B_1, B_2 and α may therefore be calculated from these indices and the well known expression for the Fresnel coefficients.

Once the Kerr component is determined, the complex Kerr rotation may be calculated from

$$\theta_k + \mathrm{i}\varepsilon_k = \frac{k}{r} \tag{7}$$

where $k \ll r$ and r is the amplitude reflectance of the whole system that may be easily calculated using the reiterative reflectance formula [21].

To determine the complex values of the Voigt parameters of the Co and Pd layers it is assumed that the value for Co (Q_{Co}) is a constant and that of the Pd varies exponentially with distance from the interface with the Co according to $Q_{\mathrm{Pd}}\mathrm{e}^{-\beta z}$. Functions other than the exponential have been tried but, within experimental error, the exponential fit is adequate. The procedure used was to fit the variations of Kerr rotation and ellipticity during the deposition of

the Pd layer in the first period. Several pairs of data points were taken and used in a regression analysis using the Marquardt–Levenberg procedure to adjust the values of Q_{Co}, Q_{Pd} and the decay constant β to fit the data. The numerical results of this calculation are given in table 1.

6. Discussion

Using the parameters of table 1 it is possible to calculate the variations of the complex Kerr effects throughout the deposition of several periods. Figure 8 shows a section of such a calculation for the first three bi-layers of a deposition. For each Co deposition the onset of the calculated magneto-optic signal has been deliberately shifted to coincide with the observed delay that occurs during the deposition of the first 0.14 nm.

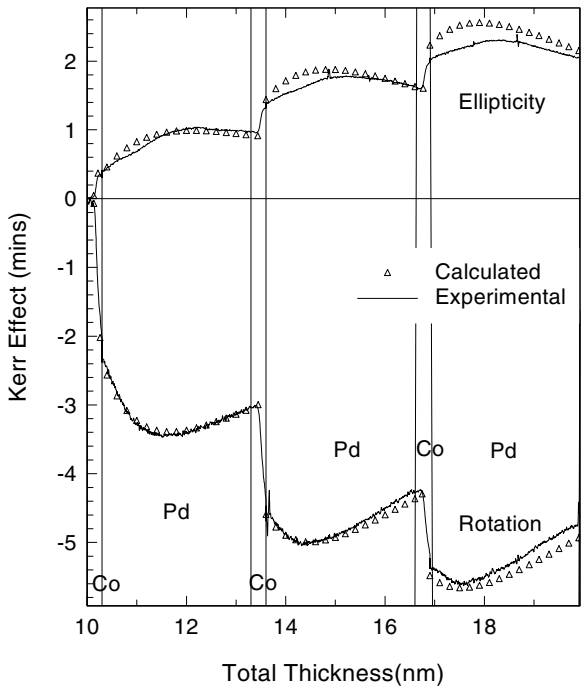

Figure 8. The measured and calculated complex polar Kerr effect during the continuous deposition of the first three Co–Pd bi-layers.

Before commenting on the comparison between the measured and calculated data it is worth pointing out the spatial variation of the modulus of the magneto-optic parameter in this type of system. This is shown schematically in figure 9 for the buffer layer and the following completed bi-layer. This variation demonstrates how the Co layer induces an exponentially varying moment in the underlying buffer layer. It similarly indicates how the moment varies in the Pd layer that lies between two completed Co layers. In this case the combination of induced moments that decay exponentially from each interface gives rise to the curve shape seen. Clearly, the $|Q|$-value for Pd is greater than that for Co, largest at the interfaces and reaches a minimum midway between the two Co layers. It is also clear that the layer thicknesses (Co/Pd//0.3/3 nm) are not optimum from the point of view of maximizing the Kerr signal from a Co–Pd multilayer since a large fraction of the Pd layer will have a small moment and therefore contribute minimally to the Kerr effect whilst having a significant effect on optical absorption.

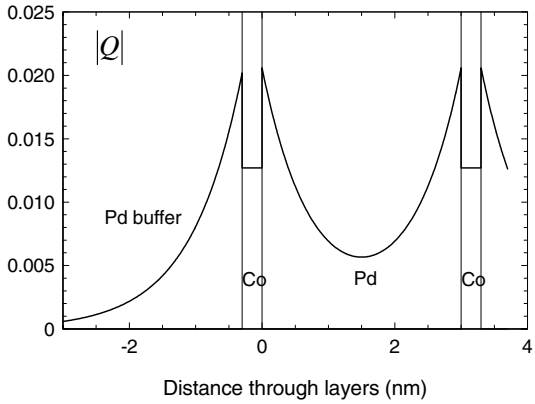

Figure 9. A spatial profile of the modulus of the magneto-optic Q-parameter as a function of distance after the deposition of the buffer layer and Co–Pd–Co.

A detailed analysis of the optimization of performance with respect to Pd thickness, based on the data in this paper, is given elsewhere [19].

Bearing in mind these distributions of magneto-optic parameters, it is now simple to understand the evolving signals seen during the deposition process. The calculated curves based on fitting the first bi-layer agree remarkably well for all three periods and this continues beyond this point. A close examination of figure 8, for the deposition of the first Co layer, shows the significant contribution to magneto-optic activity that comes about through polarization of the Pd underlayer. In the calculation, this is triggered on arrival of the first few magnetic Co atoms. As a consequence there is a very rapid and large increase in the negative Kerr rotation and a smaller positive increase in ellipticity. The details of the actual changes that are observed during the deposition of the Co monolayer are difficult to model since the precise nature of the nucleation and growth process and the way in which the ferromagnetic state switches on is unknown. However, we can estimate the contributions of Co and Pd to the measured Kerr effect. From the fitted data it is known that the contribution of the Co to the Kerr rotation is only about 20% of the total. The rest, some 80%, is due entirely to the polarization within the underlying Pd buffer layer. In the case of ellipticity the contribution of the Co is, in fact, negative despite the positive ellipticities that are observed. The reason for this is that the negative contribution of Co to the ellipticity is outweighed by a larger positive contribution that comes from the polarized Pd. The magnitude of this is about 2.2 times greater than that due to the Co. The fact that the contributions of Co and Pd to the ellipticity are of opposite sign is one of the reasons for the observed ellipticity being smaller than the rotation in the curves of figures 5 and 8. The small contribution of Co to the Kerr effect is what is expected on the basis of ultrathin-film values of Q_{Co} similarly determined for Co–Au systems and is entirely consistent with other experiments by the authors [16]. It is emphasized that when comparing the relative contributions of Co and Pd, it is problematic to use only Kerr rotation and/or ellipticity since these parameters are not intrinsic material constants and are affected by the optical environment in which a magnetic layer may find itself. Nevertheless, a more rigorous calculation based upon measured $|Q|$-values and optimized Pd layer thicknesses [19] indicates that the Co contributes about 20% of the magneto-optic activity at this wavelength. If the Co is assumed to behave as the bulk, this is increased to about 33%.

Following the details of the magneto-optic signals, after the deposition of the initial Co layer, the deposition sequence proceeds predictably and the curve shapes are reproduced very

well by the calculations that take into account the dynamically changing inhomogeneities of the Pd layers. These inhomogeneities in the magnetic moment of the Pd layer extend a considerable distance from the interface and decay exponentially with a decay constant of about 1.1 nm^{-1} from both interfaces with the Co. As the number of bi-layers increases, the calculated and experimental curves separate a little, though the general shapes of the curves are very well matched. The differences are most probably due to small systematic errors in the calculated optical and/or magneto-optical parameters. Alternatively, they could be the result of changing spatial variations in the magneto-optic parameter of the Pd layers owing to a possible deterioration in quality of the interfaces.

A final and very important detail that should not be overlooked in figure 8 is the small undulations seen in the experimental ellipticity curves, particularly in the first bi-layer, that are not seen in the calculated curves. These undulations or flattened sections are quite reproducible and clearly represent some physical process that is as yet unexplained. These effects are small and, probably for this reason, have not, to our knowledge, been seen before in Pd. However, such effects have been seen by the authors in Co–Au structures [16], where the undulations are much larger and very clear indeed. The current understanding is that, in Co–Au, the oscillations in ellipticity (and in rotation for later bi-layers or for thicker buffer layers [22]) are due to thickness-dependent spin-polarized quantum well energy levels associated with the Au layer [22–26].

To show these effects more clearly in these results we have fitted a smooth quadratic curve to the ellipticity section of the first bi-layer and subtracted this from the experimental data to produce the differential change in ellipticity, $\Delta\varepsilon_k$, over this section. The results are shown in figure 10 where oscillations in Kerr ellipticity, with a period of about 1.6 nm, can now be seen. The same periodicity also exists in the case of CoAu.

It seems that here, for the first time, we may have evidence for quantum well levels existing in ultrathin layers of Pd. It is worth noting that the reason the effects of these levels appear as oscillations in ellipticity, rather than rotation, is most probably related to the optical properties of the system that are determined by the use of a relatively thin buffer layer. This enhances the effects on ellipticity at the expense of those on rotation. Similar observations are seen for Co–Au [16]. The detailed optical and magneto-optical consequences of the quantized levels are not easily calculated in absolute terms and are certainly beyond the scope of this work.

7. Conclusions

Ellipsometry and Kerr polarimetry have been used to follow the continuous evolution of the optical and magneto-optical properties of multiple layers of Co (0.3 nm) and Pd (3 nm) in real time during their deposition by sputtering. Optical data show that the multilayered material is physically stable and may be treated as being a homogeneous medium having a single refractive index at the wavelength of 632.8 nm. Magnetic measurements showed strong perpendicular anisotropy at all stages of the deposition process once the initial monolayer of Co had been deposited. Films were therefore held in a state of magnetic saturation during data collection. Magneto-optic signals associated with the normal-incidence polar Kerr effect indicated strong polarization of Pd atoms at both Co–Pd and Pd–Co interfaces and that the modulus of the complex magneto-optic Voigt parameter and therefore the magnetic moment of the Pd decreases exponentially from the interface with a decay constant of 1.1 nm^{-1}. Theoretical simulations based on a magneto-optic theory for inhomogeneously magnetized media have allowed the determination of the ultrathin-film values of the elements of the skew-symmetric permittivity tensor that describe the optical and magneto-optical properties for both Co and Pd. The agreement between measured data and the calculated curve profiles is generally excellent,

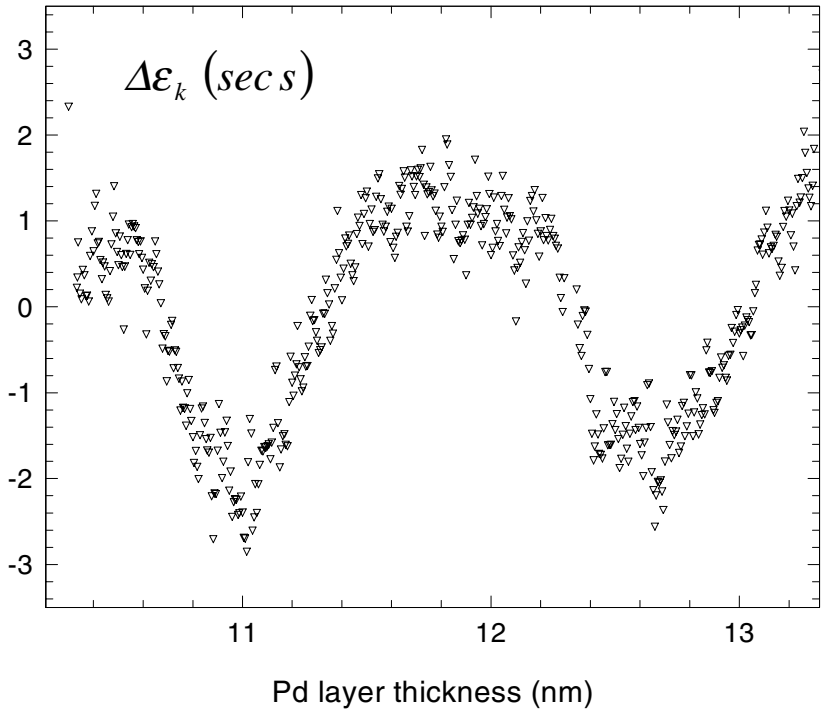

Figure 10. Oscillations in the differential Kerr ellipticity as a function of Pd layer thickness for the first bi-layer. (Spatial period: approximately 1.6 nm.)

apart from some small deviations due to distinct structure in ellipticity recorded during the deposition of Pd. This structure may result from Pd-thickness-dependent oscillations in the Kerr ellipticity. The oscillations have a spatial period of about 1.6 nm and are believed to be due to the effects of quantum well states associated with ultrathin layers of Pd. Similar effects, with the same period, have been seen before in Co–Au multilayers but have not, to our knowledge, been seen in Co–Pd. Further work at increased sensitivity is required to confirm the existence of the oscillations in Co–Pd.

Acknowledgments

The authors wish to acknowledge the support of the EPSRC through the provision of a ROPA (Reaching Our Potential Award) grant GR/L69619. The authors are also grateful to Mr T E McKenna for his able technical support on this experimentally demanding project.

Note added in proof. The authors wish to point out that in a related article [19] the value of the decay constant β for Pd was misreported as being 0.11 nm^{-1}. The correct value is 1.1 nm^{-1}.

References

[1] Zeper W B, Greidanus F J A M, Carcia P F and Fincher C R 1989 *J. Appl. Phys.* **65** 4971
[2] Atkinson R, Pahirathan S, Salter I W, Grundy P J, Tatnall C J, Lodder J C and Meng Q 1996 *J. Magn. Magn. Mater.* **162** 131

[3] Parkin S S P, More N and Roche K P 1990 *Phys. Rev. Lett.* **64** 2304
[4] Baibich M N, Broto J M, Fert A, Nguyen Van Dau F, Petroff F, Etienne P, Creuzet G, Friederich A and Chazelas J 1988 *Phys. Rev. Lett.* **61** 2472
[5] Dieny B, Speriosu V S, Parkin S S P, Gurney B A, Wilhoit D R and Mauri D 1991 *Phys. Rev.* B **43** 1297
[6] Freeman A J and Wu R Q 1992 *J. Magn. Magn. Mater.* **104–107** 1
[7] Atkinson R and Dodd P M 1997 *J. Magn. Magn. Mater.* **173** 202
[8] Uba S, Uba L, Perlov A Ya, Yaresko A N, Antonov V N and Gontarz R 1997 *J. Phys.: Condens. Matter* **9** 447
[9] Zvezdin A K and Kotov V A 1997 *Modern Magneto-Optics and Magneto-Optic Materials* (Bristol: Institute of Physics Publishing)
[10] Sato K 1981 *Japan. J. Appl. Phys.* **20** 2403
[11] Aspnes D E 1982 *Thin Solid Films* **89** 249
[12] Maxwell-Garnett J C 1904 *Phil. Trans. R. Soc.* A **203** 385
Maxwell-Garnett J C 1906 *Phil. Trans. R. Soc.* A **205** 235
[13] Hendren W R 1994 *PhD Thesis* Queen's University, Belfast, UK
[14] Atkinson R and Lissberger P H 1992 *Appl. Opt.* **31** 6076
[15] Atkinson R 1993 *J. Magn. Magn. Mater.* **124** 333
[16] Atkinson R, Didrichsen G, Hendren W R, Salter I W and Pollard R J 2000 *Phys. Rev.* B **62** 12 294
[17] Visnovsky S 1991 *Czech. J. Phys.* **41** 663
[18] Atkinson R and Kubrakov N F 1995 *Proc. R. Soc.* A **449** 205
[19] Atkinson R 2000 *J. Phys.: Condens. Matter* **12** 7735
[20] Atkinson R and Lissberger P H 1993 *J. Magn. Magn. Mater.* **118** 271
[21] Lissberger P H 1970 *Rep. Prog. Phys.* **33** 197
[22] Mégy R, Bounouh A, Suzuki Y, Beauvillain P, Bruno P, Chappert C, Lecuyer B and Veillet P 1995 *Phys. Rev.* B **51** 5586
[23] Katayama T, Suzuki Y, Hayashi M and Geerts W 1994 *J. Appl. Phys.* **75** 6360
[24] Ortega J E, Himpsel F J, Mankey G J and Willis R F 1993 *Phys. Rev.* B **47** 1540
[25] Suzuki Y, Katayama T, Bruno P, Yuasa S and Tamura E 1998 *Phys. Rev. Lett.* **80** 5200
[26] Bruno P, Suzuki Y and Chappert C 1996 *Phys. Rev.* B **53** 9214